July, 1985

Studies of Silicon-Phosphorus Bonding

Kenneth J. Dykema
Thanh N. Truong
Mark S. Gordon

preferentially at the Glu-270 portion of the intermediate instead of the cinnamoyl portion of the denatured intermediate. The intramolecular trapping requires sufficient nucleophilicity of the α-acylamino groups. The efficiency of the intramolecular reaction by the acylamino groups has not been well investigated.[31]

Although the trapping experiments failed to produce positive results, strong support for the assignment of ES′ observed in the hydrolysis of **3** to the anhydride intermediate formed by the acylation of the Glu-270 carboxylate came from the pH profile of k_{cat} for **2** or **3** (Figure 4). The k_{cat} values are essentially pH-independent over pH 5.5–9.5.[32] The breakdown of the anhydride intermediate would occur through the attack of water or hydroxide ion. The k_3 would be independent of pH unless the hydroxide path becomes significant. The pH independence of k_{cat}, therefore, is consistent with the breakdown of the anhydride intermediate mainly through water attack.

Almost all the pH profiles of k_{cat} for the CPA-catalyzed reactions reflect the ionization of a functional group with pK_a of 6–7.[14,16,28,33-37] This group, which should be in the basic form for the enzyme activity, is usually assigned to the Glu-270 carboxylate. If k_{cat} stands for the breakdown of the anhydride intermediate, however, ionization of Glu-270 should not be reflected in the pH profile of k_{cat}, as in the pH profiles for **2** and **3**.

The pH effects have been studied on the breakdown of the intermediate observed for **6** under cryoenzymological conditions. The pK_a value calculated from the observed sigmoid pH profiles was 6.5 when the temperature was extrapolated to 25 °C.[5] Since the observed intermediate was later shown to be a noncovalent complex,[7] the pK_a can be assigned to Glu-270 and the observed reaction is best described as the acylation of Glu-270.

The intermediate observed during the hydrolysis of **3** is the most stable intermediate ever reported for CPA, in terms of both the half-life ($0.693/k_3$) and the magnitude of $K_m$app. In addition, it contains a good chromophore. Thus, the intermediate is well suited for spectroscopic characterization.

Activation Thermodynamic Parameters and Solvent Isotope Effects. Usually, k_{cat} for an enzymatic reaction is contributed to by several rate constants, and, therefore, its physical meaning is not straightforward. For **2** and **3**, k_{cat} represents k_3, and its temperature dependence and D_2O effect are related solely to the deacylation of ES′.

The activation entropy change (Table III) is not large, suggesting that the unimolecular breakdown of ES′ involves little changes in conformational freedom.

Among the substrates listed in Table IV, k_{cat} for *N*-(*N*-benzoylglycyl)-L-Phe (BGP) likely represents the acylation of Glu-270 (k_2). For **2** and **3**, the observed solvent isotope effect is rather small, being similar to that of BGP, for the nucleophilic attack of water at an acyl center. For the rest of the substrates listed in Table IV, k_{cat} is a complex quantity. No obvious trend is seen among the values of the solvent isotope effect. Instead, the data of Table IV demonstrate the limitation of solvent isotope effects in the mechanistic study of enzymes. Even with simple organic reactions, the solvent isotope effect does not necessarily differentiate the nucleophilic and general base mechanisms.[38] In enzymatic reactions, the contribution of the secondary isotope effects intrinsic to the enzyme would be even more significant.[39]

Effects of α-Acylamino Groups on Kinetic Parameters. The values of the rate parameters for **7** (Table II) fit (not shown) the Hammett plot[21] obtained for various para-substituted derivatives of **4**. Thus, the *p*-acetylamino group exerts only electronic effects. On the other hand, the α-acylamino groups of **1–3** lead to remarkably small k_{cat} and $K_m$app. When α-acylamino groups are attached to the cinnamoyl peptide substrates, k_{cat} is enhanced while $K_m$app is affected only slightly.

Several differences in the behavior of CPA toward ester and peptide substrates, such as the effects of metal substitution, inhibitors, or chemical modification, have been reported. This was explained in terms of different mechanisms[34,40,41] for esters and peptides but was also accounted for by a single mechanism[28,42] with different rate-determining steps. Similarly, the effects of the α-acylamino groups on the kinetic parameters for esters and for peptides can be explained in terms of a single mechanism of eq 9.

For peptides **8–11**, the acyl-CPA intermediate (ES′) does not accumulate and the acylation step is likely to be rate-determining. Thus, case B of Table V holds for **8–11**. Cases A and C of Table V apply to esters **4–7** and **1–3**, respectively. Thus, the effects of the α-acylamino groups on the kinetic parameters of these substrates are explained by assuming that k_2 is raised, k_3 is lowered, and K_m or K_s is little affected by the introduction of the α-acylamino groups.

Acknowledgment. This work was supported by a grant from the Korea Science and Engineering Foundation.

(30) Sugimoto, T.; Kaiser, E. T. *J. Org. Chem.* **1978**, *43*, 3311.
(31) Kirby, A. J.; Fersht, A. R. *Prog. Bioorg. Chem.* **1971**, *1*, 1.
(32) The slightly lower k_{cat} at pH 5.5 can be ascribed to the partial protonation of a His residue coordinating to the active-site zinc ion and the consequent partial dissociation of the zinc ion.[33]
(33) Auld, D. S.; Vallee, B. L. *Biochemistry* **1971**, *10*, 2892.
(34) Auld, D. S.; Vallee, B. L. *Biochemistry* **1970**, *9*, 4352.
(35) Carson, F. W.; Kaiser, E. T. *J. Am. Chem. Soc.* **1964**, *86*, 2922.
(36) Bunting, J. W.; Kabir, S. H. *Biochim. Biophy. Acta* **1978**, *527*, 98.
(37) Spratt, T. E.; Sugimoto, T.; Kaiser, E. T. *J. Am. Chem. Soc.* **1983**, *103*, 3679.
(38) Bender, M. L.; Pollock, E. J.; Neveu, M. C. *J. Am. Chem. Soc.* **1962**, *84*, 595.
(39) Jencks, W. P. "Catalysis in Chemistry and Enzymology"; McGraw-Hill: New York, 1969; Chapter 4.
(40) Auld, D. S.; Holmquist, B. *Biochemistry* **1974**, *13*, 4355.
(41) Auld, D. S.; Vallee, B. L. *Biochemistry* **1970**, *9*, 602.
(42) Cleland, W. W. *Adv. Enzymol. Relat. Areas Mol. Biol.* **1977**, *45*, 273.

Studies of Silicon–Phosphorus Bonding

Kenneth J. Dykema, Thanh N. Truong, and Mark S. Gordon*

Contribution from the Department of Chemistry, North Dakota State University, Fargo, North Dakota 58105. *Received September 10, 1984*

Abstract: Ab initio calculations are presented for several species containing a silicon–phosphorus bond. The types of bonding studied include "normal" single, double, and triple bonds, as well as an ylide-like structure. The latter is found to be much less strongly bound than the carbon analogue, with a smaller stretching force constant than that in silylphosphine. The insertions of silylene into the phosphine bond and of phosphinosilylene into H_2 are discussed, with the former being illustrated using localized molecular orbitals along the intrinsic reaction coordinate (IRC). Silylene to silene isomerizations in both the closed-shell singlet and the lowest triplet states of $SiPH_3$ are analyzed in the same manner.

I. Introduction

As part of an ongoing program investigating the nature of bonding of silicon in a variety of molecular environments, the present paper presents an analysis of the bonding between silicon and phosphorus in a variety of prototypical environments. These include "normal" triple (I), double (II), and single (III) bonds, as well as the apparently hypervalent ylide (IV).

0002-7863/85/1507-4535$01.50/0

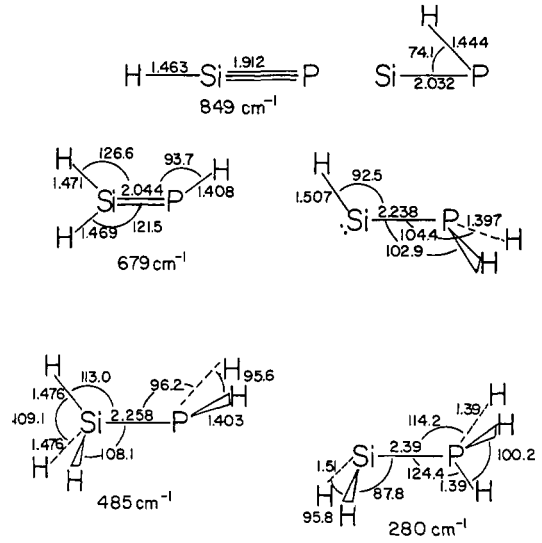

Figure 1. 3-21G* structures for closed-shell Si–P molecules: bond lengths in ångströms, angles in degrees.

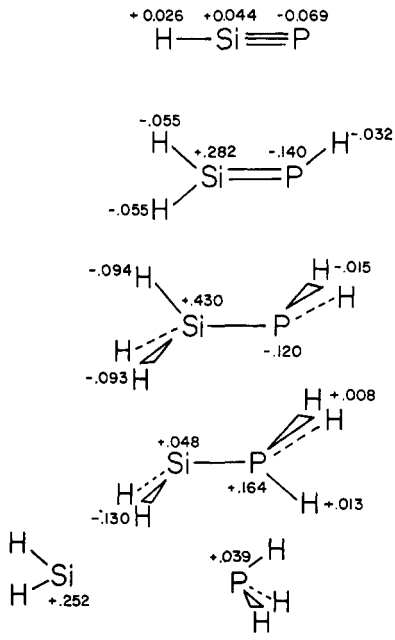

Figure 2. Figure 2. Net (Mulliken) atomic charge distributions in closed-shell Si–P molecules.

$$\underset{\text{I}}{HSi{\equiv}P} \qquad \underset{\text{II}}{H_2Si{=}PH} \qquad \underset{\text{III}}{H_3Si{-}PH_2} \qquad \underset{\text{IV}}{H_2Si{-}PH_3}$$

In addition to the analysis of the molecular and electronic structures of I–IV, the isomerization pathways connecting II with the phosphino-substituted silylene (V) in both closed-shell and triplet states and silylphosphine (III) with IV will be discussed.

$$\underset{\text{V}}{HSi{-}PH_2}$$

Finally, the reaction pathways for the insertions of singlet silylene into phosphine (eq 1) and phosphinosilylene into molecular hydrogen (eq 2) will be presented.

$$H_2Si + PH_3 \rightarrow H_3Si\text{-}PH_2 \qquad (1)$$

$$H_2PSiH + H_2 \rightarrow H_3Si\text{-}PH_2 \qquad (2)$$

Previous calculations have dealt with carbon–phosphorus bonding,[1-5] but to our knowledge, little attention has been paid thus far to the interaction between silicon and phosphorus. Similarly, the only experimental data available for the species and properties considered here are the structural and internal rotation data for silylphosphine.[6]

II. Computational Methodologies

All molecular structures, including those at saddle points, were predicted at the SCF level with the 3-21G* basis set.[7] The closed shells were treated with the usual RHF method,[8] while the UHF approach[9] was used for the triplet states. Geometry optimizations and detection of transition states were carried out with the methodology due to Schlegel.[10]

Once a transition state has been detected, the reaction may be traced along the intrinsic reaction coordinate (IRC)[11,12] forward to products and back to reactants. This procedure has been carried out for the isomerizations of the singlet and triplet states of II to the corresponding silylenes and for reaction 1, using an improved and automated process for determining the IRC.[13] To provide an illustration of the progress of these reactions, Boys localized molecular orbitals[14] have been generated at selected points along each path and for each of the structures I–IV. For the prediction of accurate energetics, single-point calculations were carried out with the 6-31G* basis set,[15] augmented by third-order Moller–Plesset perturbation theory (MP3).[16] The computer codes used for the calculations were modified versions of GAMESS[17] and GAUSSIAN 80.[18]

III. Results and Discussion

A. Molecular Structures and Si–P Bonding. The 3-21G* geometries for the stable species I–V are shown in Figure 1. The four structures I–IV have positive definite force constant matrices at this level, and the corresponding Si–P stretching frequencies are also listed in the figure. Experimental data are available only for silylphosphine,[6] and even here the information is rather sketchy. What experimental data are known for this molecule are in good agreement with the computational results. The calculated structures and vibrational frequencies for the nominally "normal" single, double, and triple bonds (I–III) display the expected trends, with decreasing bond lengths and increasing frequencies as the unsaturation increases.

In light of the fact that silaethyne[19,20] and disilaethyne[21-24] are

(1) D. J. Mitchell, S. Wolfe, and H. B. Schlegel, *Can. J. Chem.*, **59**, 3280 (1981).
(2) I. Absar and J. R. Van Wazer, *J. Am. Chem. Soc.*, **94**, 2382 (1972).
(3) H. Lischka, *J. Am. Chem. Soc.*, **99**, 353 (1977).
(4) G. Trinquier and J.-P. Malrieu, *J. Am. Chem. Soc.*, **101**, 7169 (1979).
(5) C. Thomson, *J. Chem. Soc., Chem. Commun.*, 322 (1977).
(6) R. Varma, K. R. Ramaprasad, and J. F. Nelson, *J. Chem. Phys.*, **63**, 915 (1975); C. Glidewell, P. M. Pinder, A. G. Robiette, and G. M. Sheldrick, *J. Chem. Soc., Dalton Trans.*, 1402 (1972).
(7) W. J. Pietro, M. M. Francl, W. J. Hehre, D. J. DeFrees, J. A. Pople, and J. S. Binkley, *J. Am. Chem. Soc.*, **104**, 3039 (1982).
(8) C. C. J. Roothaan, *Rev. Mod. Phys.*, **23**, 69 (1951).
(9) J. A. Pople and R. K. Nesbet, *J. Chem. Phys.*, **22**, 571 (1954).
(10) H. B. Schlegel, *J. Comput. Chem.*, **3**, 214, (1982).
(11) K. Fukui, *J. Phys. Chem.*, **74**, 4161 (1970).
(12) K. Ishida, K. Morokuma, and A. Komornicki, *J. Chem. Phys.*, **66**, 2153 (1977).
(13) M. Dupuis, M. W. Schmidt, and M. S. Gordon, *J. Am. Chem. Soc.*, **107**, 2585 (1985).
(14) J. M. Foster and S. F. Boys, *Rev. Mod. Phys.*, **32**, 300 (1960).
(15) M. M. Francl, W. J. Pietro, W. J. Hehre, M. S. Gordon, D. J. DeFrees, and J. A. Pople, *J. Chem. Phys.* **77**, 3654 (1982).
(16) J. A. Pople, J. S. Binkley, and R. Seeger, *Int. J. Quantum Chem. Symp.*, **10**, 1 (1976).
(17) J. S. Binkley, R. A. Whiteside, R. Krishnan, R. Seeger, D. J. *DeFrees*, H. B. Schlegel, S. Topiol, L. R. Kahn, and J. A. Pople, *QCPE*, **138**, 406 (1981).
(18) M. Dupuis, D. Spangler, and J. J. Wendoloski, NRCC Software Catalog, 1980, 1, Program QG01.
(19) M. S. Gordon and J. A. Pople, *J. Am. Chem. Soc.*, **103**, 2945 (1981).
(20) M. R. Hoffmann, Y. Yoshioka, and H. F. Schaefer III, *J. Am. Chem. Soc.*, **105**, 1084 (1983).
(21) L. C. Snyder, Z. R. Wasserman, and J. W. Moskowitz, *Int. J. Quantum Chem.*, **21**, 565 (1982).
(22) F. Kawai, T. Noro, A. Murakami, and K. Ohno, *Chem. Phys. Lett.* **92**, 479 (1982).

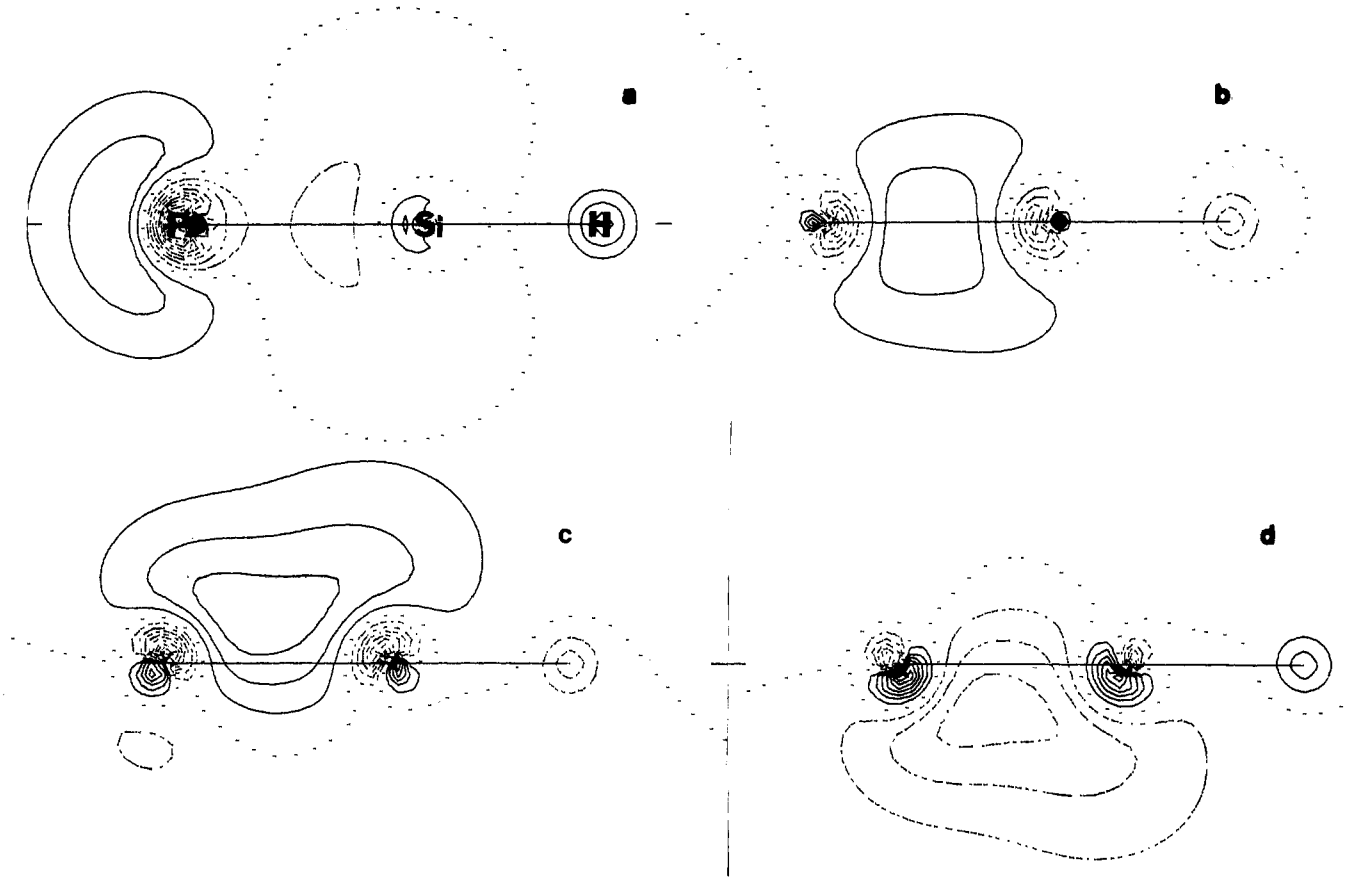

Figure 3. Boys localized silicon–phosphorus bond orbitals in HSiP: (a) P lone pair; (b)–(d) banana bonds.

Table I. Total Energies (Hartrees)

molecules	SCF/3-21G*	SCF/6-31G*	MP3/6-31G*
$SiH_2 + PH_3$	−629.266 94	−632.448 05	−632.658 30
HSiP	−626.964 78	−630.130 79	−630.341 26
SiPH	−626.982 60	−630.153 08	−630.356 31
$^1H_2SiPH$	−628.161 75	−631.333 73	−631.546 85
$^3H_2SiPH$	−628.145 10	−631.321 32	−631.502 17
$^1HSiPH_2$	−628.146 60	−631.321 71	−631.525 92
$^3HSiPH_2$	−628.135 00	−631.309 87	−631.494 62
SiH_3PH_2	−629.357 98	−632.534 81	−632.750 41
SiH_2PH_3	−629.293 94	−632.473 66	−632.694 60
saddle points			
HSiP ↔ SiPH	−626.945 18	−630.115 26	−630.314 56
PH insertion[a]	−629.239 17	−632.417 54	−632.655 83
HH insertion[b]	−629.231 23	−632.409 04	−632.647 70
ylide[c]	−629.206 57	−632.385 05	−632.629 10
$^1H_2SiPH$[c]	−628.086 25	−631.250 61	−631.482 78
$^3H_2SiPH$[c]	−628.074 28	−631.250 61	−631.448 25

[a] Insertion of silylene into phosphine. [b] Insertion of phosphino silylene into H_2. [c] Hydrogen shift.

both predicted to be nonlinear, it is interesting that HSiP has a stable linear structure. Even so, we find the SiPH isomer to be lower in energy (see below), with a strongly bent structure. In contrast, closed-shell planar $H_2Si{=}PH$ is found to be 13 kcal/mol lower in energy than its silylene isomer at the MP3/6-31G* level of accuracy. Because atoms in the third row of the periodic table often form unusual bonding structures, a search for additional H_3PSi isomers was carried out with the 3-21G* basis set. At this computational level, stable structures with positive definite force constant matrices do exist for both H_3PSi and H_3SiP in C_s symmetry. However, using MP3/6-31G* single points at the 3-21G* geometries, these structures are predicted to be 47.2 and 31.1 kcal/mol above the silylene structure, respectively. A bridged P–H–SiH_2 structure was found, but it has one imaginary frequency, and all attempts to detect a stable structure with two bridging hydrogens failed. In the following section discussion will be limited to the two most stable isomers—the silene and silylene.

The silicon ylide IV is a bit of an anomaly relative to its carbon analogue. The latter is found[1-3] to be stronger than a "normal" single bond because of π-back bonding from the carbene lone pair. It is clear from Figure 1 that the Si–P bond in IV is very weak, with a considerably longer bond length and smaller stretching frequency than those in its isomer silylphosphine. Furthermore, the internal geometries of the phosphine and silylene fragments are virtually the same in the complex as they are at infinite separation. A partial rationale for this is provided by the Mulliken populations presented in Figure 2. The formation of the ylide from silylene and phosphine results in a shift in electron density from phosphorus to silicon, as expected in such species. Since silicon is much more electropositive than carbon, however, the former is much less able to accomodate such an accumulation of negative charge. Thus, the formation of the ylide is energetically less favorable than in the carbon analogue. In addition, following Trinquier and Malrieu,[4] the greater 3s–3p splitting in silicon relative to the 2s–2p splitting in carbon will render formation of a double bond from SiH_2 more difficult than from CH_2.

The bonding in these species is further illustrated in Figures 3–6, in which selected Boys localized molecular orbitals (LMO's) are displayed for the four structures under discussion. In HSiP (Figure 3) there are three equivalent "banana" bonds connecting the two heavy atoms and a (roughly) sp lone pair on the phosphorus. Similarly, H_2SiPH (Figure 4) has two equivalent banana bonds and an approximately sp^2 phosphorus lone pair, while silylphosphine (Figure 5) exhibits a σ SiP bond and an sp^3 lone pair on phosphorus. All LMO's have been projected into the same (molecular) plane for ease of comparison. Note that, as one would expect, the number of contours between Si and P increases from the triple to the double to the single bond. The LMO's for the ylide structure (Figure 6) are rather different from those of the

(23) J. S. Binkley, *J. Am. Chem. Soc.*, **106**, 603 (1984).
(24) H. Lischka and H. Kohler, *J. Am. Chem. Soc.*, **105**, 6646 (1983).

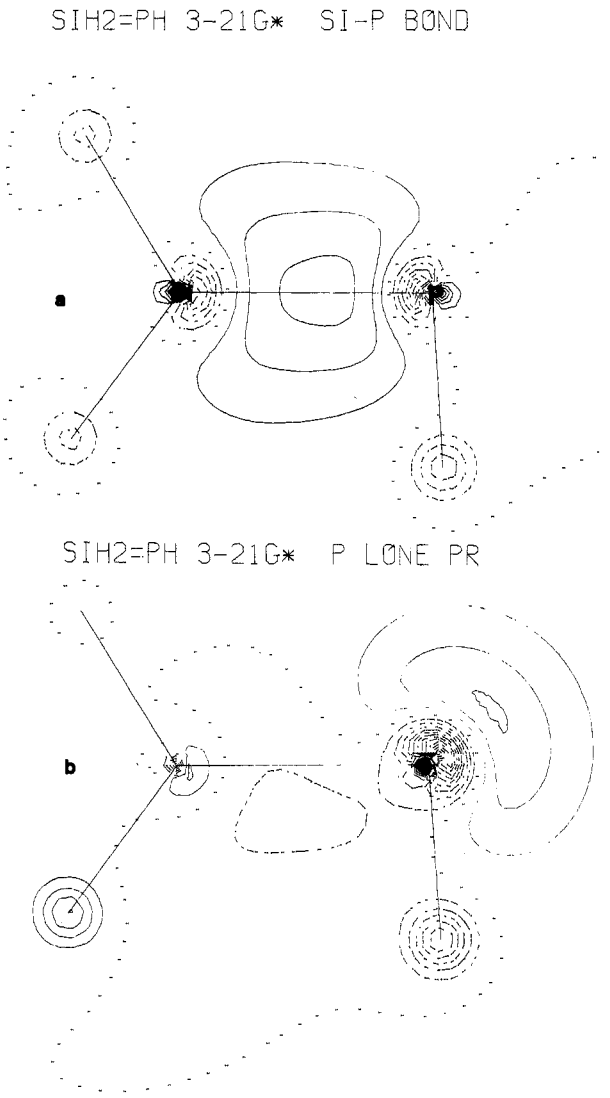

Figure 4. Boys localized silicon–phosphorus bond orbitals in H_2SiPH: (a) banana bond; (b) lone pair.

corresponding carbon analogue. In the latter, one finds two equivalent banana bonds,[25] indicative of a significant degree of multiple bonding. In contrast, silylenephosphorane has a highly polarized Si–P bond with very little electron density on silicon and a silicon lone pair with no discernible back-bonding onto phosphorus.

B. Chemical Reactions. The energetics for the primary reactions considered in this work are summarized in Figure 7, and the corresponding transition-state structures are displayed in Figure 8. For the purpose of clarity, the internal rotation of silylphosphine and the 1,2-hydrogen shift from HSiP have been omitted from Figure 7, and these will be discussed below. The total energies for all species considered here are listed in Table I.

The global minimum on the ground-state potential energy surface of $SiPH_5$ is silylphosphine in its all staggered configuration. The eclipsed structure is shown in Figure 8d. There are no significant structural changes upon internal rotation, and the (MP3/6-31G*//3-21G*) calculated internal rotation barrier of 1.48 kcal/mol is in excellent agreement with the experimental value of 1.535 kcal/mol.[6]

Formation of the ylide apparently occurs with no barrier[4] and with an energy decrease of about 22 kcal/mol at the MP3/6-31G* level of computation. The closest comparison between these results

(25) M. W. Schmidt and M. S. Gordon, unpublished results.

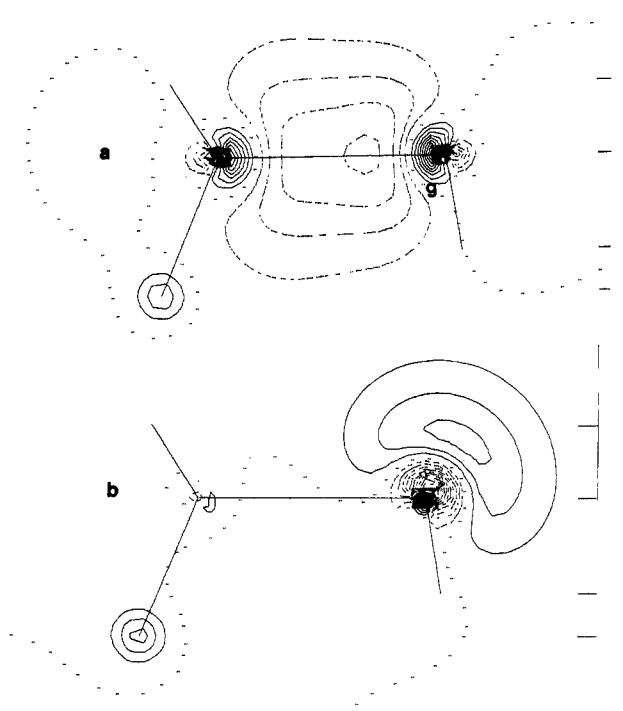

Figure 5. Boys localized silicon–phosphorus bond orbitals in SiH_3–PH_2: (a) Si–P bond; (b) P lone pair.

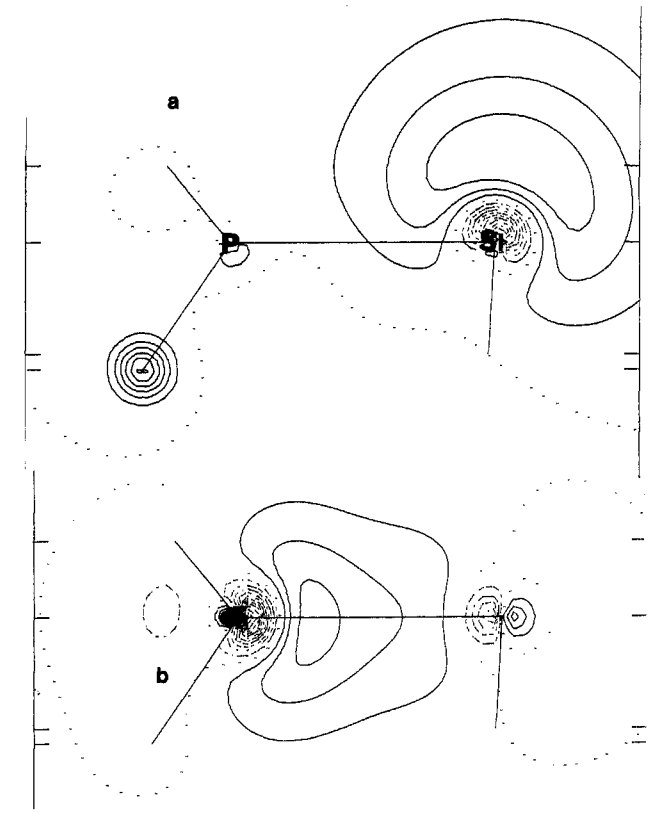

Figure 6. Boys localized silicon–phosphorus bond orbitals in SiH_2–PH_3: (a) Si lone pair; (b) P–Si bond.

and the corresponding reaction for the carbon compound is provided by the 4-31G* SCF calculations by Mitchell, Wolfe, and Schlegel.[1] These authors find methylenephosphorane to be stabilized by about 47 kcal/mol relative to singlet carbene and phosphine. The corresponding 3-21G* SCF value is 17 kcal/mol for silylenephosphorane. This comparison reinforces the notion expressed earlier that the silicon compound is much more weakly bound than its carbon analogue. It is important to point out that

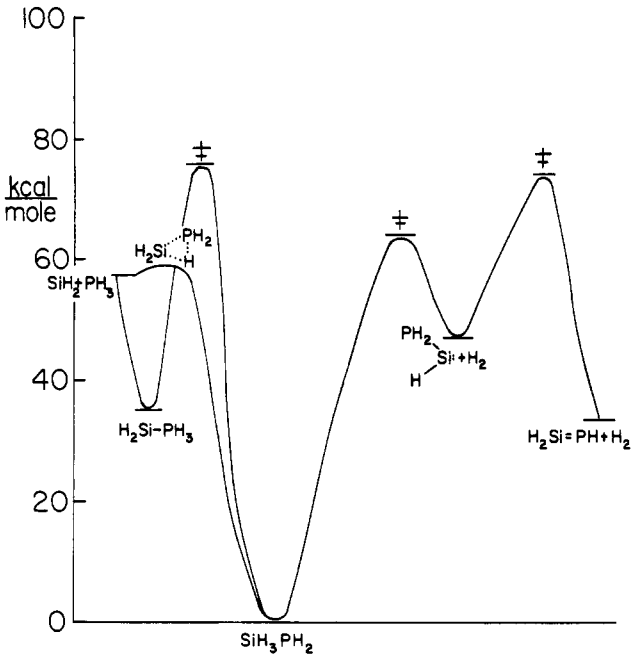

Figure 7. Energy schematic for silicon–phosphorus reactions. Dotted line corresponds to triplet state.

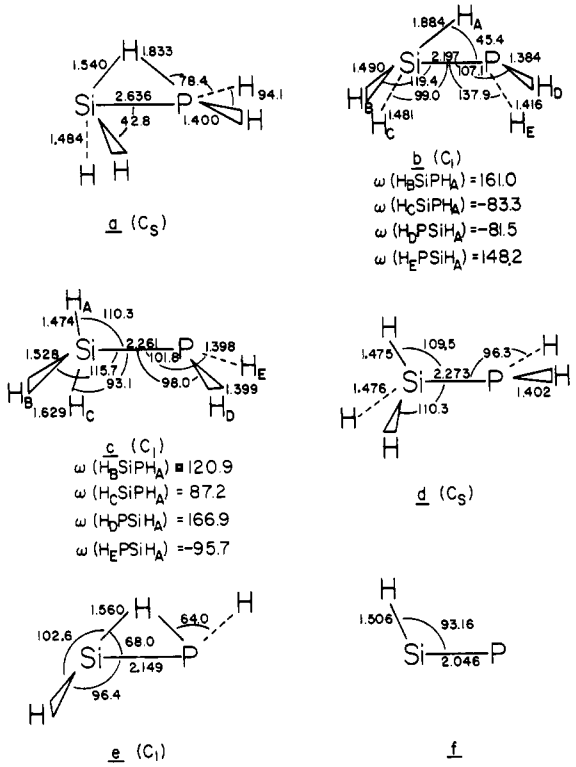

Figure 8. Closed-shell transition-state structures: (a) insertion of SiH_2 into PH_3; (b) 1,2-hydrogen shift; (c) insertion of phosphinosilylene into hydrogen; (d) eclipsed silylphosphine; (e) closed-shell 1,2-shift; (f) 1,2-shift (bond lengths in ågströms, angles in degrees).

some of this 30-kcal/mol difference in stability is a result of the inherently lower stability of the Si–P bond in general. For example, the SCF stabilization energy of silylphosphine, again relative to silylene and phosphine, is only 57.3 kcal/mol compared to 106.3 kcal/mol for methylphosphine.[1]

Returning to Figure 7, it may be seen that the barrier to insertion of silylene to form silylphosphine is less than 2.0 kcal/mol. This very small barrier has been noted previously[26] and is in agreement with experimental evidence that such insertions occur rapidly.[27] It is not unlikely that this barrier will disappear altogether under further refinement of the calculations. In contrast, the barrier to the 1,2-hydrogen shift from silylenephosphorane to silylphosphine is a substantial 40 kcal/mol. However, it should be noted that the very low barrier to the silylene insertion into phosphine provides a potentially lower energy alternative route from the ylide to silylphosphine. It may be seen in Figure 8b that the transition-state structure for this reaction is somewhat unusual in that the Si–P bond length is shorter than that in either of the two stable species. In view of the relative energies of the two isomers, it is not surprising that the transition state lies closer to the ylide structure.

The insertion of silylene into a phosphine PH bond may be analyzed further by investigating the corresponding intrinsic reaction coordinate. The most interesting (3-21G* SCF) localized orbitals at selected points along the IRC are shown in Figure 9. The transformation of the reaction PH bond into the newly formed Si–P σ bond in silyl phosphine is illustrated in Figure 9a. Here one sees a three-center bond in the transition state (center frame), with significant electron density remaining on the reacting hydrogen. In Figure 9b, the silylene lone pair increases its electron density on the reacting hydrogen and becomes a well-formed Si-H bond orbital by the transition state (center frame in the figure).

The more interesting features of the structural data for the insertion reaction along the IRC are summarized in Figure 10. As noted in earlier works on insertion reactions,[28,29] the initial attack of the silylene occurs at large Si–H–P angles, but this angle closes up as the reaction proceeds. By the transition state (point 0 in the figure) this angle has closed to 102.4°. The silylene hydrogens are in a staggered arrangement with respect to the phosphine throughout the reaction, with the very small H–Si–P angle opening up as the reaction proceeds. The last part of the reaction to occur is the movement of the reacting hydrogen to form its final HSiP angle. While the bond lengths are all close to their final values by point F, the angle is still only 71.4°. This permits some retention of the H——P interaction late into the exit channel.

Silylphosphine can also eliminate H_2 to form a phosphino-substituted silylene. As shown in Figure 7, the barrier to this elimination is quite large (65 kcal/mol), and the reverse insertion barrier is a significant 17.5 kcal/mol. This latter barrier is twice as large as that for the unsubstituted insertion at a comparable level of theory.[28,30] The ground state of the phosphinosilylene is predicted to be a closed-shell singlet, with the triplet lying about 20 kcal/mol higher in energy. It is likely that this singlet–triplet splitting is overestimated by about 50% at this level of theory, since the analogous splitting for the unsubstituted silylene (15.7 kcal/mol) is too high by 4–5 kcal/mol.[31]

The singlet and triplet isomerization hypersurfaces from phosphinosilylene to the corresponding SiH_2PH species are nearly parallel, with the triplet remaining higher in energy throughout the path. The closed-shell transition state structure is shown in Figure 8, while all of the triplet structures are shown in Figure 11. As expected, all of the triplet structures are nonplanar. The Boys localized orbitals at selected points along the closed-shell IRC are illustrated in Figure 12. One of the two equivalent Si–P "banana" bonds in H_2SiPH (not shown) transforms into the Si–P σ bond in the silylene. As illustrated in Figure 12a, the second banana bond distorts rapidly into the silicon lone pair in the silylene. Indeed, the lone pair is already well formed at the transition state (center frame in the figure). Finally, the transformation of the Si–H bond through a three-center bond in the transition state region to a P-H bond at the silylene is depicted in Figure 12b.

(26) K. Raghavachari, J. Chandrasekhar, M. S. Gordon, and K. J. Dykema, *J. Am. Chem. Soc.*, **106**, 5853 (1984).
(27) G. R. Langford, D. C. Moody, and J. D. Odom, *Inorg. Chem.*, **14**, 134 (1975).
(28) M. S. Gordon and D. R. Gano, *J. Am. Chem. Soc.*, **106**, 5421 (1984).
(29) F. Anwari and M. S. Gordon, *Isr. J. Chem.*, **23**, 129 (1983).
(30) M. S. Gordon, *J. Chem. Soc., Chem. Commun.*, 890 (1981).
(31) M. S. Gordon, unpublished results.

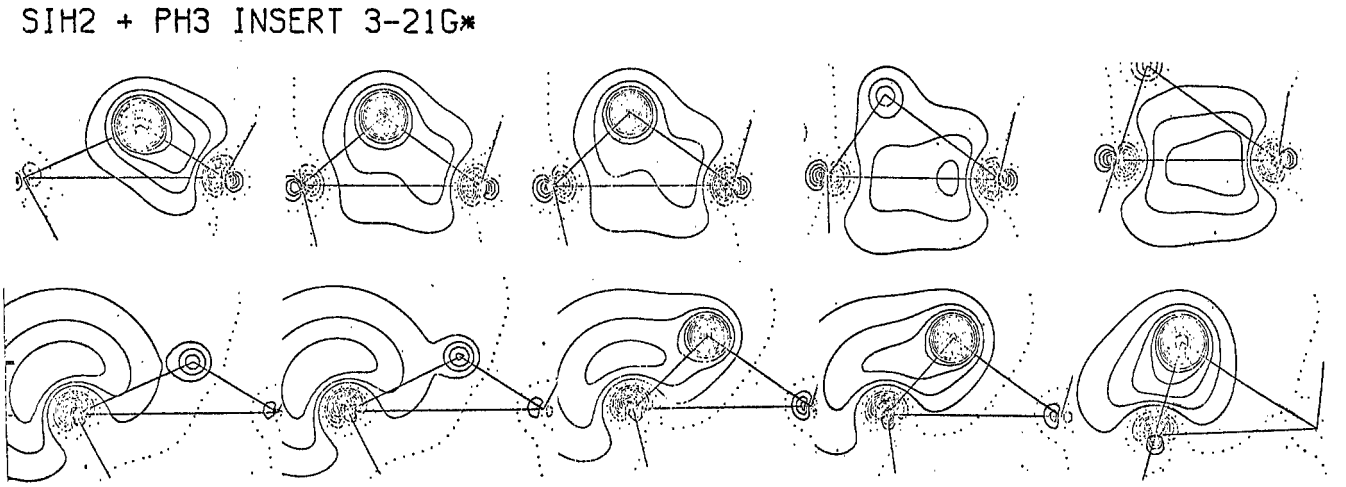

Figure 9. Boys localized orbitals along the IRC for the SiH_2 insertion into phosphine: (a) transformation from P–H bond to Si–P bond; (b) transformation from silylene lone pair to Si–H bond (central frame is transition state).

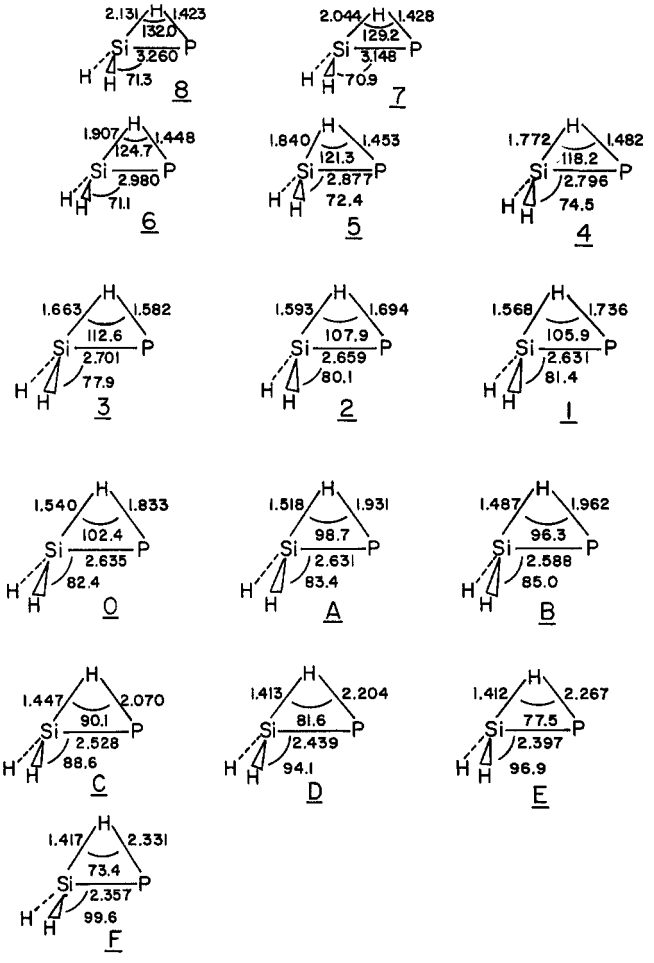

Figure 10. Structures along the SiH_2 + PH_3 IRC: bond lengths in ångströms, angles in degrees.

Similar pictures are displayed for the α and β triplet orbitals along the UHF IRC in Figure 13. Since the triplet is nonplanar throughout the path, the Si–P bond (not shown) remains σ and simply distorts slightly as the active hydrogen migrates. In the α space (Figures 13a and 13b) the SiH bond transforms into the silicon lone pair, while the phosphorus lone pair becomes the P–H bond. Because there is only one corresponding β MO (Figure 13c: there is no β lone pair), the Si–H bond goes through a three-center transition state en route to becoming the P–H bond at the silylene end.

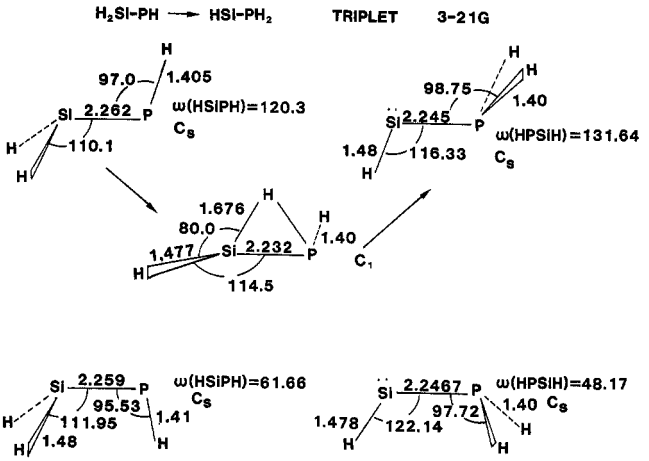

Figure 11. Triplet structures: bond lengths in ångströms, angles in degrees.

Finally, note that despite the fact that linear HSiP is found to have a positive definite harmonic force field at the 3-21G* SCF level, the global minimum on this surface is predicted to be the HPSi isomer shown in Figure 1. This rather unusual, highly bent structure is found to be 9.4 kcal/mol lower in energy than HSiP at the MP3/6-31G* level. The structure of the transition state for this, 1,2-hydrogen shift is shown in Figure 8. This structure is also somewhat unusual in that the Si–P bond length is longer at the transition state than in either of the two isomers. The MP3/6-31G* barrier to isomerization from HSiP to HPSi is predicted to be 16.8 kcal/mol.

IV. Conclusions

The major conclusions which may be drawn from this work are as follows:

(1) The nominally normal single (pyramidal), double (planar), and triple (linear) Si–P bonds are found to be stable with positive definite harmonic force fields. Despite the fact that the triply bound structure has a more stable (silylidene) isomer, these results are in contrast with those found earlier for Si–Si and Si–C multiple bonds. The linear triple bonds for both of these species are unstable,[19-24] and the Si–Si double bond is found to be nonplanar as well.

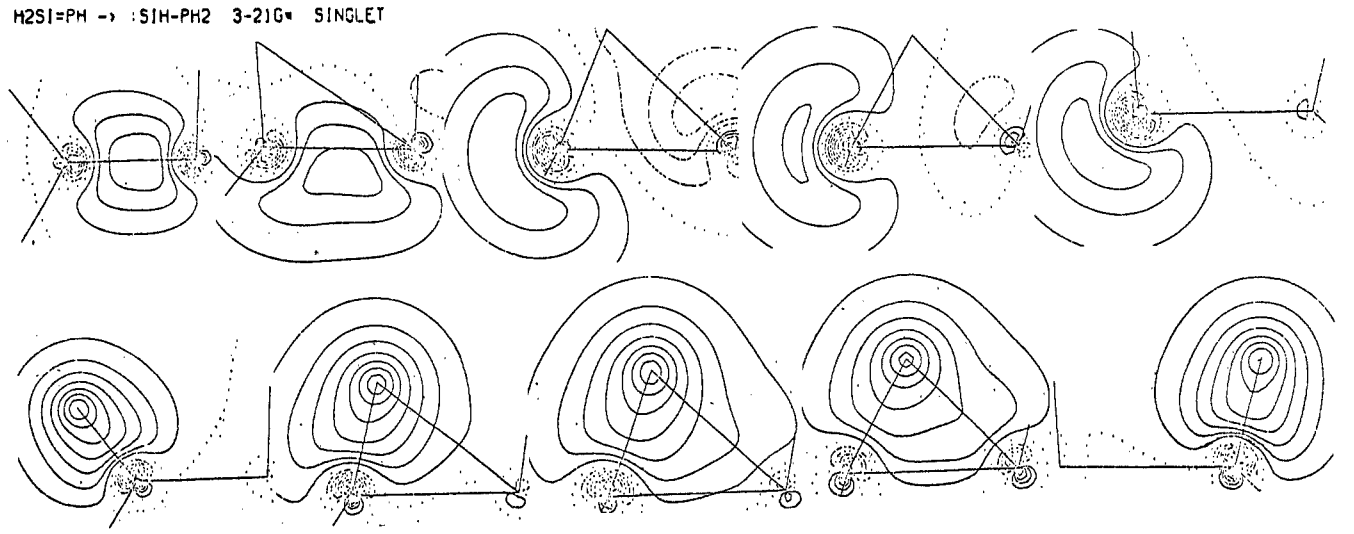

Figure 12. Boys localized orbitals along the IRC for the singlet isomerization from H_2SiPH to $HSiPH_2$: (a) transformation from Si–P banana bond to Si lone pair; (b) transformation from Si–H bond to PH bond (central frame is transition state).

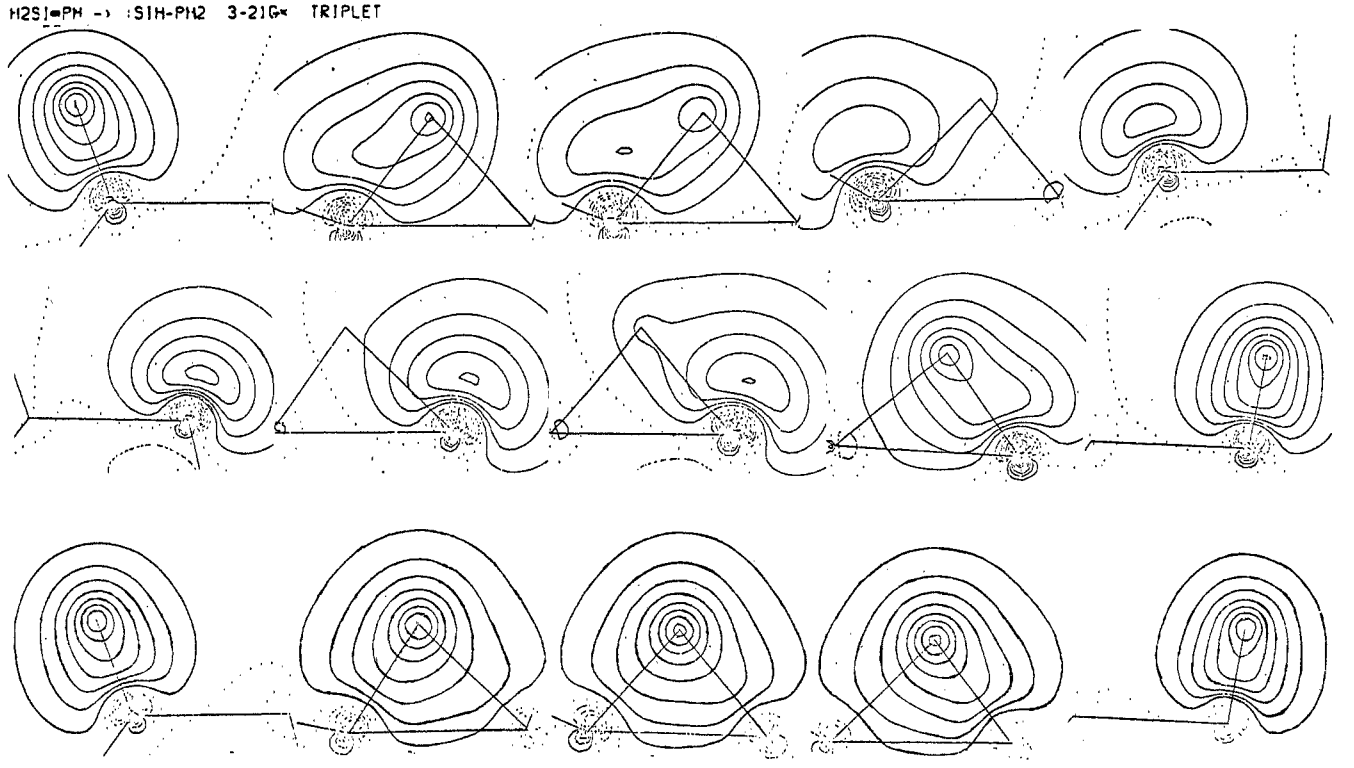

Figure 13. Boys localized orbitals along the IRC for the triplet isomerization from H_2SiPH to $HSiPH_2$: (a) transformation from α Si–H bond to Si lone pair; (b) transformation from α P lone pair to P–H bond; (c) transformation from β Si–H bond to P-H bond (central frame is transition state).

(2) Because of the electropositive nature of silicon, the silylene ylide is found to be much less stable than its carbon analogue, with a bond strength much less than the corrsponding single bond.

(3) The barrier to the insertion of silylene into the P–H bond of phosphine is predicted to be just 2 kcal/mol, while the barrier to insertion of phosphinosilylene into H_2 is about 17 kcal/mol. The former result is consistent with experimental evidence.[27]

(4) The 40-kcal/mol barrier for the singlet 1,2-hydrogen shift from phosphinesilene to the corresponding silylene is similar to the barriers found for other 1,2-shifts.[32] The potential energy surface for the triplet is higher than and approximately parallels the singlet surface.

Acknowledgment. This work was supported by the donors to the Petroleum Research Fund (No. 13035-AC6), administered by the American Chemical Society, and by the Air Force Office of Scientific Research (AFOSR 82-0190). The computer time made available by the North Dakota State University Computer Center is gratefully acknowledged.

(32) See, for example, H. F. Schaefer III, *Acct. Chem. Res.*, **15**, 283 (1982).

Registry No. II, 95187-06-7; III, 14616-47-8; V, 96667-04-8; H_2Si, 13825-90-6; PH_3, 7803-51-2; H_2, 1333-74-0; Si, 7440-21-3; P, 7723-14-0.